KFKI-1978-9

A. ZAWADOWSKI

BOUND EXCITATIONS IN He^4

Hungarian Academy of Sciences

CENTRAL
RESEARCH
INSTITUTE FOR
PHYSICS

BUDAPEST

KFKI-1978-9

BOUND EXCITATIONS IN He^4

A. Zawadowski
Central Research Institute for Physics
H-1525 Budapest P.O.B. 49 Hungary

Lectures given at the International "Etore Majorana" School of Low Temperature Physics Erice, June 1977.

HU ISSN 0368 5330
ISBN 963 371 375 7

ABSTRACT

The excitation spectrum of liquid He^4 exhibits two extremes as the roton minimum and the maxon maximum. These parts of the excitation spetrum with large density of states play important roles in several aspects of the liquid He^4 as in thermal properties, in the formation of the light scattering spectra and in the neutron scattering distribution. The different mechanism for light scattering on He^4 are discussed and it is found that mainly roton pairs with symmetry of d-type excited. By Raman scattering the two roton excitation spectrum can be measured; the shape of the spectrum, however, can not be interpreted as the excitation of two noninteracting rotons with total momentum zero. The experimental data are explained by assuming an attractive roton-roton interaction which results in the formation of bound roton pairs. The lineshape is discussed from the theoretical point of view in detail. The concept of bound roton pairs is extended to pairs with arbitrary total momentum. Considering further evidences for the attractive roton-roton interaction the temperature dependence of the single roton lifetime and energy are studied. The hybridization of the single excitation and the two roton branches is discussed in order to explain the neutron scettering distribution.

АННОТАЦИЯ

Спектр возбуждений жидкого He^4 имеет две экстремальные точки ротонный минимум и максонный максимум. Эти части спектра возбуждений с большой плотностью состояний играют важную роль в поведении жидкого He^4, а именно в термических свойствах, в сформировании спектра рассеяния света и в распределении негронного рассеянияв статье обсуждаются разные механизмы для рассеяния света в жидком He^4 и получается,что в основном возбуждаются ротонные пары имеющие симметрию типа "d". С помощью рассеяния Рамана двухротонный спектр возбуждений может быть измерен, но форма спектра не может быть объяснена как возбуждение двух невзаимодействующих ротона полным импульсом равным нулью. Экспериментальные данные объясняются с помощью предположения притяжающего взаимодействия между ротонами, которые в последствии ведет к возникновению связанным ротонным парам. Форма спектра дискутируется с точки зрения теории подробно. Концепция о связанных ротонных парах распостраняется на пары с любым полным импульсом. Учитывая дальнейшие доказательства о притяжающем взаимодействии между ротанами изучается температурная зависимость времени жизни и энергии одного ротона. С целью объяснить распределение нейтронного рассеяния Обсуждается гибридизация элементарных возбуждений с двумя ротонными ветвями.

KIVONAT

A He^4 gerjesztési spektrumának két extremális helye van a roton minimum és a maxon maximum. A gerjesztési spektrumnak ezek a nagy állapotsürüségü részei több szempontból is lényeges szerepet játszanak a folyékony He^4 tulajdonságait tekintve, mint pl. termikus viselkedés, a fény és neutron szórási spektrumok szempontjából. A különböző fényszórási mechanizmusokat tárgyaljuk, és azt találjuk, hogy főként d-szimmetriáju roton párok gerjesztődnek. A Raman szórás segitségével a két roton gerjesztési spektrum mérhető; a spektrum alakja azonban nem értelmezendő mint két nemkölcsönható, zérus teljes impulzusu rotonpár gerjesztése. A kisérleti adatokat egy csomó roton-roton kölcsönhatás segitségével értelmezzük, amely két roton kötött állapotra vezet. A vonal alakot részletesen vizsgáltuk elméleti szempontból. A két roton kötött állapotát kiterjesztjük tetszőleges teljes impulzusra. A vonzó roton-roton kölcsönhatás további alátámasztása céljából a roton élettartamának és energiájának hőmérsékletfüggését vizsgáljuk. Az egyszeres gerjesztési és két roton gerjesztési spektrum hibridizációját tárgyaljuk azért, hogy értelmezzük a neutronszórási spektrumot.

I. Introduction

In order to explain the peculiar thermodynamical properties of superfluid He^4 thirty six years ago Landau [1] proposed the excitation spectrum shown in Fig. 1. Although, Landau's theory describes correctly the overall behavior of the spectrum, in recent years numerous new details have been found experimentally and explained theoretically on the basis of the interaction between excitations. Two lecture series of this school are dealing with these new features, thus Greytak in his lecture is considering the light scattering experiments and Cowley is presenting the results of neutron spectroscopy. The aim of the present lectures is to provide some theoretical background concentrating on the role of pair excitations.

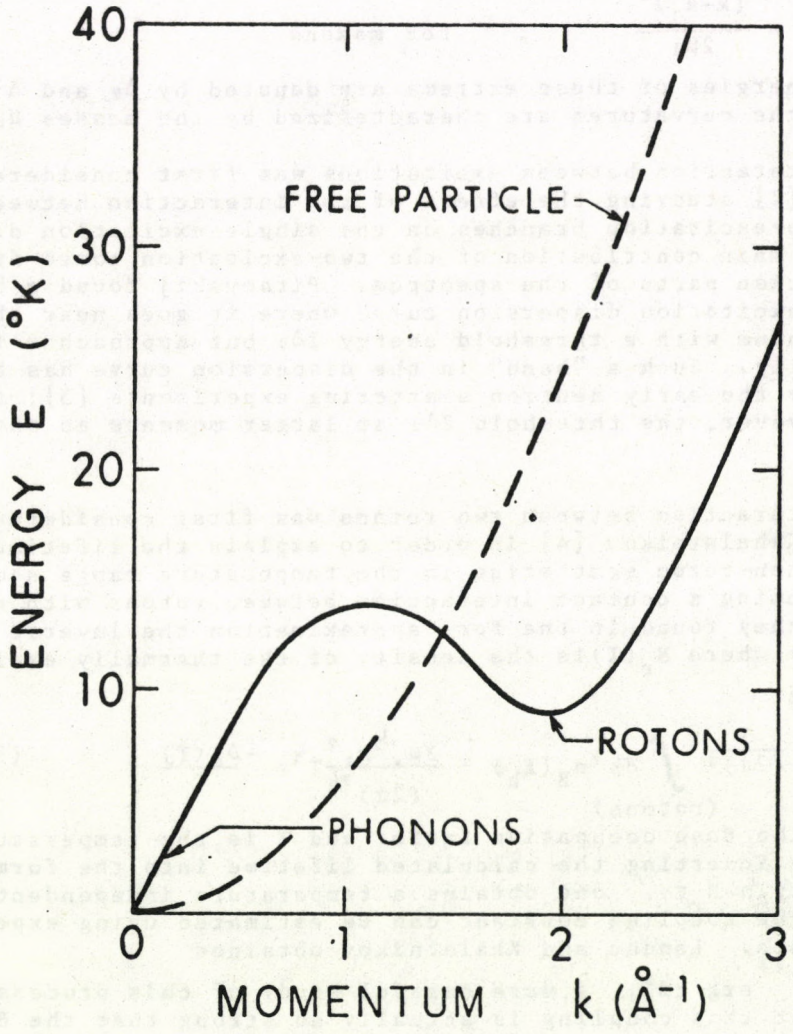

Figure 1. The excitation spectrum of superfluid helium proposed by Landau showing the roton minimum in contrast to the free particle behavior.

Landau's spectrum is different from the free particle spectrum in many respects; namely it exhibits a phonon like linear dispersion at low momenta, the roton minimum, and a maximum between these two regions where the excitations have been called maxons recently. The roton and the maxon parts of the dispersion curve are of particular importance because they contribute to the density of states to a large extent. The dispersion curve E(k) in these regions can be approximated as

$$E_k = \Delta_0 + \frac{(k-k_0)^2}{2\mu_0} \quad , \quad \text{for rotons} \qquad (1)$$

and

$$E_k = \Delta_0 - \frac{(k-k_1)^2}{2\mu_1} \quad , \quad \text{for maxons} \qquad (2)$$

where the energies of these extrema are denoted by Δ_0 and Δ_1, respectively and the curvatures are characterized by the masses μ_0 and μ_j.

The interaction between excitations was first considered by Pitaevskij [2] studying the effect of the interaction between the one- and two-excitation branches on the single-excitation dispersion curve. The main contribution of the two-excitation comes from the roton and maxon parts of the spectrum. Pitaevskij found a bending of the one-excitation dispersion curve where it goes near the two-roton continuum with a threshold energy $2\Delta_0$ but approaches it asymptotically. Such a "bend" in the dispersion curve has been demonstrated by the early neutron scattering experiments [3]; the curve exceeds, however, the threshold $2\Delta_0$ at larger moments as shown in Figure 2.

The interaction between two rotons was first considered by Landau and Kahalatnikov [4] in order to explain the lifetime coming from the roton-roton scattering in the temperature range above 0.8 K^0. Assuming a contact interaction between rotons with coupling constant g_4 they found in the Born approximation the inverse lifetime $1/\tau_r \sim g_4 N_r(T)$ where $N_r(T)$ is the density of the thermally excited rotons, thus

$$N_r(T) = \frac{1}{(2\pi)^3} \int_{(\text{rotons})} dk^3 n_B(E_k) \simeq \frac{2\mu_0^{1/2} k_0^2}{(2\pi)^{3/2}} T^{1/2} e^{-\frac{\Delta_0(T)}{T}} \quad , \qquad (3)$$

where n_B is the Bose occupation factor and T is the temperature. Moreover, by inserting the calculated lifetime into the formula of the viscosity $\eta \sim N_r \tau_r$, one obtains a temperature independent viscosity and the coupling constant can be estimated using experimental viscosity data. Landau and Khalatnikov obtained $|g_4| \approx 2.6\ 10^{-38}$ erg cm^3. A more careful study of this process shows, however, that this coupling is actually so strong that the Born approximation cannot be applied and the experimental results cannot be explained in this way, but this was not realized at that time.

The fast development of the field of the two roton excitations started with the new light scattering experiments of Greytak and Yan[5] in 1969, which became feasible due to application of laser beams. In these experiments two rotons have opposite momenta. Furthermore, the new neutron scattering data of Woods and Cowley[6] contain information on the neutron spectra above the two-roton

energy. These developments on the experimental side stimulated further theoretical studies.

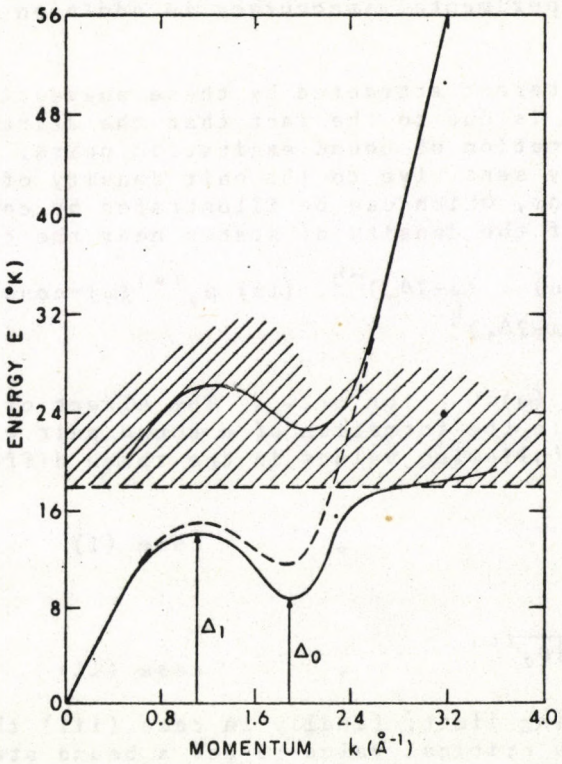

Figure 2. Neutron scattering data for liquid helium yield the two-branch spectrum shown by the solid lines. The two roton continuum is indicated by the shaded region.

In the experiments mentioned before the two-excitation spectrum is reflected in a direct or indirect way, which spectrum is defined in the case of noninteracting excitations as

$$\rho_2^{(0)}(K,\omega) = \frac{1}{2}\left(\frac{1}{2\pi}\right)^3 \int \delta(\omega - E_k - E_{K-k})\, d^3K \qquad (4)$$

where the factor 1/2 comes from the Bose statistics. As we will see later this density of states is singular at the two-roton and two-maxon thresholds (at energies $2\Delta_1$ and Δ_1) for total momentum K=0, but it behaves like a step function at the thresholds for larger K.

In the light scattering experiments with negligible momentum transfer one would expect a spectrum typical for K=o, exhibiting two singularities. The experiments [5], however, confirmed the existence of the first peak roughly at $2\Delta_0$ but not of the second one at $2\Delta_1$. These suprising experimental findings stimulated Iwamoto [7] and independently Ruvalds and Zawadowski [8], who suggested that the interaction between two rotons or two maxons is attractive and the spectrum is strongly modified by that . The success of this theory

encouraged the analysis of the neutron scattering data [9, 10], where the two roton spectrum must show up, but with finite total momentum $K \neq 0$, and in these investigations the energy region above $2\Delta_0$ was included into a theoretical treatment similar to the one proposed by Pitaevskij [2]. It has turned out, however, that in respect to the roton-roton interaction, the early neutron data are less conclusive, because of the experimental inaccuracy in addition to the theoretical difficulties.

The great interest attracted by these suggestions on the roton-roton interaction is due to the fact that the attractive coupling may result in the formation of bound excitation pairs. That bound state, of course, is very sensitive to the pair density of the noninteracting excitations, which can be illustrated by considering three different types of the density of states near the threshold $2\Delta_0$ as (i) $\rho_2^{(0)}(\omega) \sim (\omega - 2\Delta_0)^{-\frac{1}{2}}$, (ii) $\rho_2^{(0)}(\omega) = \text{constant}$ (iii) $\rho_2^{(0)}(\omega) \sim (\omega - 2\Delta_0)^{\frac{1}{2}}$

for $\omega > 2\Delta_0$ and $\rho_2(\omega) \equiv 0$ for $\omega < 2\Delta_0$. The effect of the attractive interaction g_4 is in the formation of a bound pair with binding energy E_B which has the following values in the three different cases

$$E_B \sim |g_4|^2 \quad , \quad \text{case (i)} \tag{5a}$$

and

$$E_B \sim e^{-\frac{1}{2|g_4|\rho_2^{(0)}}} \quad , \quad \text{case (ii)} \tag{5b}$$

in the week coupling limit; finally in case (iii) the coupling must be stronger than a critical value to get a bound state. These results show that the larger is the density of states at the threshold the stronger is the binding.

The first two of these three cases are realized in He^4 by roton pairs with total momentum $K=0$ and $K \neq 0$. The third case may appear in the two phonon spectrum of an anharmonic crystal.

The remainder of this lecture is organized in the following way. In section II the mechanism of light scattering is discussed with respect to the two-roton excitation, and the effect of the bound roton pairs on the Raman spectrum is left to section III. The further consequences of the attractive roton-roton interaction as the temperature dependence of the energy and of the lifetime of rotons are discussed in section IV. The spectrum at finite momenta and the neutron scattering experiments are the subject of section V, and the final discussion and conclusions are left to section VI.

II. Mechanism of light scattering on pair excitations

The main feature of the light scattering experiments is that the wavelength of the light is very large compared to the interatomic spacing "a", thus the momentum transfer to the target is very small in units of $2\pi/a$. In the Brillouis scattering the light excites only one phonon-like excitation and as the energy and momentum of this excitation is very small, the excited phonon can be regarded as a macroscopic density fluctuation. There is, however, another possibility, namely, the Raman scattering in which two excitations

are created with antiparallel momenta whose absolute values are approximately the same. In case of a liquid, a pair of arbitrary excitation is large enough (see Figure 3). It was first suggested by Halley [11]in 1968 that the Raman scattering on liquid He^4 is a useful tool to investigate the spectrum of elementary excitations. Considering different pairs the largest density of states can be expected for two rotons and two maxons, furthermore, the pair density must be considerable smaller for two phonons. As it will be discussed in the next section the interaction between excitations in the created final state may essentialy modify the two-excitation density of states.

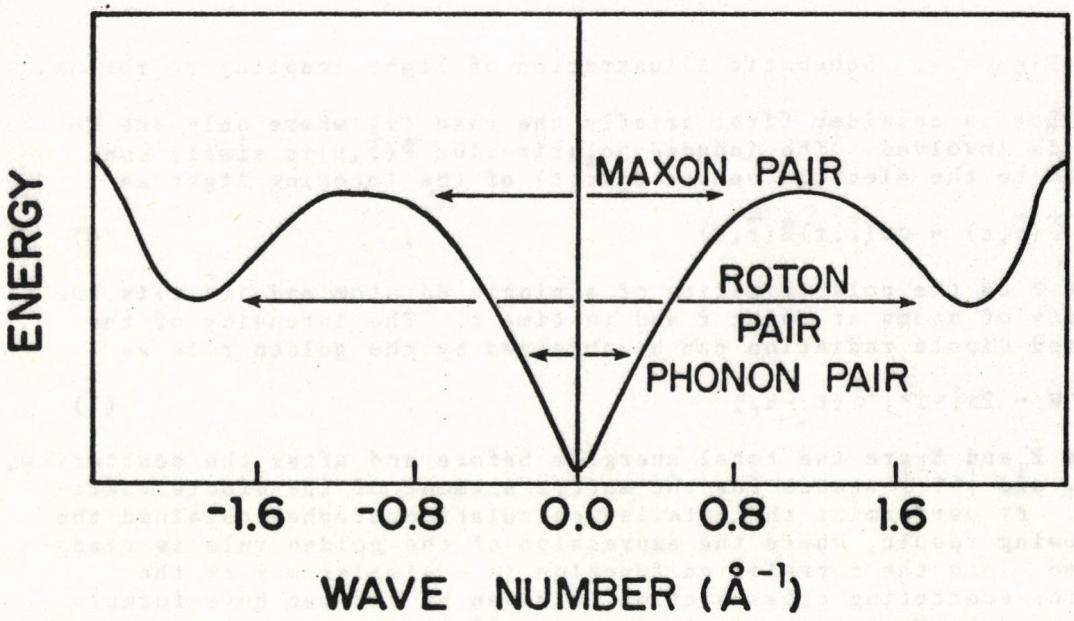

Figure 3. Excitation pairs with zero total momentum which contribute to the second order Raman scattering.

The detailed theory of the mechanism of light scattering has been worked out by Stephens [12]. The light is scattered by the density fluctuations, but this scattering is exceptionally weak in the case of He^4, because the polarizibility σ of a He atom is small. Basically, there are two different ways in which light is scattered

(i) The incoming light beam polarizes a He atom and the induced dipolemoment emits the scattered light.

(ii) The light polarizes a He atom and the created dipole field interacts with another atom by polarizing it and that induced dipole moment is the source of the emitted light.

These two processes are depicted in Fig. 4 where k_o, ω_o and $k' = k_o - k, \omega' = \omega_o$ -ware standing for the momenta and frequencies of the incoming and outgoing light and the energy and momentum transfer to the material are denoted by ω and k, respectively.

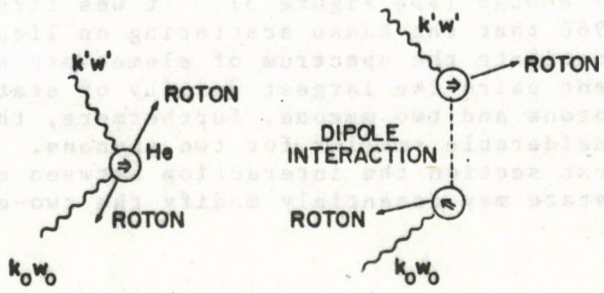

Figure 4. Schematic illustration of light coupling to rotons.

Let us consider first briefly the case (i) where only one He atom is involved. The induced polarization $\vec{P}(\vec{r},t)$ is simply connected to the electric vector $\vec{E}_o(\vec{r},t)$ of the incoming light as

$$\vec{P}(\vec{r},t) = \sigma\rho(\vec{r},t)\vec{E}(\vec{r},t) \quad , \qquad (6)$$

where σ is the polarizibility of a single He atom and $\rho(\vec{r},t)$ is the density of atoms at point $\vec{r}$ and in time t. The intensity of the emitted dipole radiation can be obtained by the golden rule as

$$W = 2\pi|\langle T\rangle|^2\delta(E_i - E_f) \quad , \qquad (7)$$

where E_i and E_f are the total energies before and after the scattering, resp. and $|\langle T\rangle|$ stands for the matrix element of the dipole radiation. By performing the detailed calculation Stephen obtained the following result, where the expression of the golden rule is transformed into the correlation function in a similar way as the neutron scattering cross section is given by the van Hove formula discussed by Cowley in his lecture, see(2.4),

$$W^{(i)} \sim \sigma^2 \left(\frac{\omega\varrho}{c}\right)^4 \left(\vec{E}\cdot\vec{E}_o\right) S\left(K,\omega\right) \quad , \qquad (8)$$

where $\vec{E}_o$ and $\vec{E}_1$ are the polarization vectors of the incoming and outgoing light, c is the speed of the light. Furthermore, the dynamical structure factor is given by the Fourier transform of the density-density correlation function as

$$S(K,\omega) = \int d^3\vec{r}\,dt\exp(-i\vec{k}\cdot\vec{r} + i\omega t)S(\vec{r},t) \quad , \qquad (9)$$

where

$$S(r_1-r_2,t_1-t_2) = \langle\rho(r_1t_1)\,\rho(r_2t_2)\rangle \quad . \qquad (10)$$

This result is very similar to the expressions (2.3) and (2.4) of Cowley's lecture. As it has been discussed there, $S(k,\omega)$ consists of the single-excitation peak with weight factor $Z(k)$ at energy E_k and of the continuous part $S^{II}(k,\omega)$ due to the multiple-excitations, thus

$$S(K,\omega) = Z(K)\delta(\omega - E_k) + S^{II}(K,\omega) \qquad (11)$$

In the case of light scattering the single excitation corresponds to the Brillouin scattering, while $S^{II}(k,w)$ contains among others the contribution of the pair-excitations.

The second mechani m (ii) can be discussed in a similar way. The difference in this case is that two He^4 atoms are involved in the scattering. They are interacting with dipole radiation which propagates with the speed of light, thus from the point of view of the liquid this interaction can be taken as an instantaneous one. Therefore, the scattering amplitude contains a product of two density operators with equal time and of weight factor determined by the dipole interaction (more precisely the Green's function of the dipole field). Stephen's detailed calculation leads to the following result

$$W^{(ii)} \simeq \sigma^4 \frac{\omega_0^4}{c} \frac{3}{5}\left(1 + \frac{1}{3}(\vec{E}_0\cdot\vec{E}_1)^2\right)\frac{1}{(2\pi)^4}\int d^3\vec{k}\,d^3\vec{k}'\,d\omega P_2(\cos\Theta_{kk'}) \times$$

$$g(k)g(k')S_2(k,k',\omega) \quad , \qquad (12)$$

where $S_2(k=0,\omega)$ is the Fourier transform of the two density correlation function

$$S(k,k',\omega) = \frac{1}{2\pi}\int dt e^{-i\omega(t-t')}\langle\rho(k,t)\rho(k',t')\rho(k,t')\rho(-k,t')\rangle \quad . \qquad (13)$$

The relative position of the two atoms involved in the scattering amplitude is characterized by the static pair correlation function $g(r)$ which tells us the probability that two atoms can be found in a distance r, and the Fourier transform $g(k)$ of $g(r)$ appears in the expression above. Finally, $P_2(\cos\Theta_{kk'})$ is the Legendre polynomial where $\Theta_{kk'}$ is the scattering angle.

The roton pair wave function is characterized by additional quantum numbers. Assuming that the total momentum is zero the quantum numbers are those of the rotational group, namely l and m. As in case (i) the excitation mechanism is independent of the momentum distribution of the toton pair, the symmetry of the excited pair must be s-like (l=0). In the second case (ii), however, the two He atoms are interacting by dipole radiation thus the excited pair must have the same symmetry as the interaction, namely d-like (l=2) and this is responsible for the appearance of the Legendre function on the right hand side of (12).

It may be mentioned that there is a term due to the interference between the two mechanisms (i) and (ii). The amplitude of the mixed process is weak because it must be proportional to the measure of breaking of the rotational symmetry K^2 which is small and it is usually neglected. In the limit K=0 the symmetry of the pairs excited with the two different mechanisms is different, thus the interference does not occur (see [13] for further discussion).

The next problem to be discussed is the intensity ratio of the different processes. In case (i) the problem is to estimate the weight of the two roton or maxon states in $S(k,\omega)$. It has been shown by Miller, Pines and Nozieres [14] that contribution to

$S^{II}(k,\omega)$ is proportional to K^4. This can be explained easily. At zero temperature we have

$$S(K,\omega) = \sum_n |\langle n|\rho_k|o\rangle|^2 \delta(\omega - E_k) \tag{14}$$

where n denotes the excited states with energy E_n. Furthermore, the matrix element of the Fourier transform of the continuity equation is

$$i\omega\langle|\rho_k(\omega)|o\rangle = k\langle n|\dot{J}_k(\omega)|o\rangle \tag{15a}$$

from where, as the matrix of the current operator is proportional to K,

$$\langle n|\rho_k(\omega)|o\rangle \sim \frac{K^2}{\omega} \tag{15b}$$

follows where the energy ω corresponds to the pairs $\omega \sim 2\Delta_0$. Thus the contribution of two rotons or maxons to $S(K,\omega)$ is proportional to K^4,

$$S^{II}(K,\omega) \sim K^4 \qquad \text{for} \qquad \omega \simeq 2\Delta_0 . \tag{15c}$$

The amplitude of the K^4 term can not be taken from the theory because of the nonexistence of sufficient theory for real He^4, however, it is known from the neutron data, see p. 1160 in [16]. Using that proportionality factor and Stephen's theory [12] the ratio of Raman scattering with mechanism (i) to Brillouin scattering is far below the observable intensity. Turning to the mechanism (ii), the expressions given by eqs. (12) and (13) should be estimated. In the noninteracting case the correlation function $S_2(k,k',\omega)$ describes the propagation of two rotons, and it can be evaluated using the excitation spectrum measured by neutron scattering as will be seen in the following and g(k) can be taken from X-ray scattering data. Using these data a ratio can be obtained [17] which is in good agreement with the ratio of Raman and Brillouin scatterings experimentally found by Woerner and Greytak [16]to be 3.4×10^{-4}. The lineshape will be the subject of the main part of our further discussion. It may be mentioned that Stephen's first estimation gave a ratio larger by a factor 10, because he used a continuum model in which a function f(r) is introduced in order to avoid selfpolarization of He atoms instead of using g(r). This function f(r) is unity if r>a ("a" is the atomic radius) and is zero otherwise. This function f(r) looks however, very much like g(r) if "a" is replaced by 2a on the basis that two atomic centres can not be nearer than the diameter of an atom.

Another general feature of Stephen's result is that it predicts the dependence of the Raman scattering cross section on the angle between the polarizations of the incident and scattered light through the factor

$$1 + \frac{1}{3}(\vec{E}_o \cdot \vec{E}_1)^2 ,$$

in the expression [13], which agrees very well with the experimental results [16]. This agreement supports the d-symmetry of the interaction between He^4 atoms and that means that a possible s-like overlapping interaction plays a negligible role. In the case of noninteracting excitations the energy dependence of the Raman spectrum can easily be obtained by factorizing the correlation function $S_2(k,k',\omega)$ as

$$S_2(k,k',\omega) = \left[\delta(k-k')+\delta(k+k')\right]\int d\omega' S(k,\omega')S(-k,\omega-\omega') \quad , \qquad (16)$$

where the density operators with different time arguments are paired and the additional third term proportional to $\delta(\omega)$ is omitted. Using (11) for $S(k,\omega)$ and ignoring the continuous part $S^{II}(k,\omega)$ one obtains

$$S(k,k',\omega) = \left[\delta(k-k')+\delta(k+k')\right] Z^2(k)\delta(\omega-2E_k) \quad , \qquad (17)$$

and inserting this result into (12), the final expression for the Raman scattering is

$$W_{Raman} = \sigma^4 \left(\frac{\omega_0}{c}\right)^4 \frac{3}{5}\left(1 + \frac{1}{3}(\vec{E}_0\vec{E}_1)\right)^2 \frac{1}{(2\pi)^4}\int d^3k\ Z^2(k)g^2(k)\delta(\omega-2E_k) \quad , \qquad (18)$$

In a smaller range of energy ($\omega \sim 2\Delta_0$) where $Z(k)$ and $g(k)$ are smoothly varying $Z(k) \sim Z(k_0)$ and $g(k) \sim g(k_0)$ the right hand side of (17) is simply proportional to the density of states for the pair excitations

$$W_{Raman} \sim g^2(k)Z^2(k)\rho_2(K=0,\omega) \qquad (19)$$

In the noninteracting case the function $\rho_2^{(0)}$ given by (4) can be evaluated using expressions (1) and (2) for the energies of rotons and maxons, resp., with the result

$$\rho^2(K=0,\omega) = \left(\frac{k_0}{2\pi}\right)^2 \left(\frac{\mu_0}{\omega-2\Delta_0}\right)^{1/2} \quad \text{for rotons} \qquad (20a)$$

$$\rho_2^{(0)}(K=0,\omega) = \left(\frac{k_1}{2\pi}\right)^2 \left(\frac{\mu_1}{\omega-2\Delta_1}\right)^{1/2} \quad \text{for maxons} \qquad (20b)$$

these expressions are singular at $\omega \sim 2\Delta_0$ and $\omega \sim 2\Delta_1$ respectively; furthermore, the phonons give a small contribution which in the approximation $E_k \sim sk$,

$$\rho_2^{(0)}(K=0,\omega) \sim \frac{1}{32\pi^2 s^3}\ \omega^2 \quad , \qquad (20c)$$

where s is the sound velocity$_{(o)}$.

The joint density of states ρ_2 is shown in Fig. 5 where all of these three contributions are taken into account. Considering the Raman spectrum one should expect square root singularities at twice of the roton energy and of the maxon energy. Greytak and Yan's first experimental results[5] are shown in Fig. 6 with the noninteracting pair excitation spectrum corrected by the factor $Z^2(k)\ g^2(k)$, see (11). The absence of the two maxon peak and the somewhat stronger appearance of the two roton peak can not be explained by the non-interacting spectrum. Ruvalds and Zawadowski[8] and independtly Iwamoto[7] have pointed out that the interaction between excitations to be discussed in the next section could be responsible for that discrepancy.

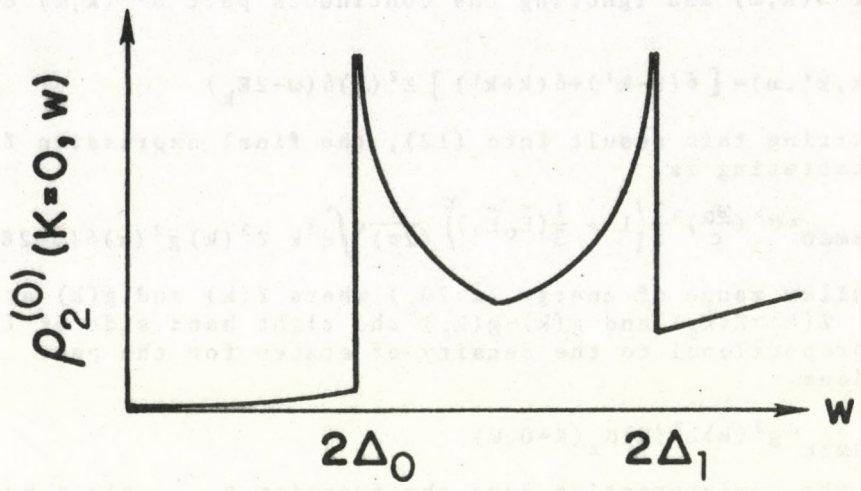

Figure 5. Two-excitation density of states showing singularities due to roton and maxon pairs along with the smooth background of the phonon continuum.

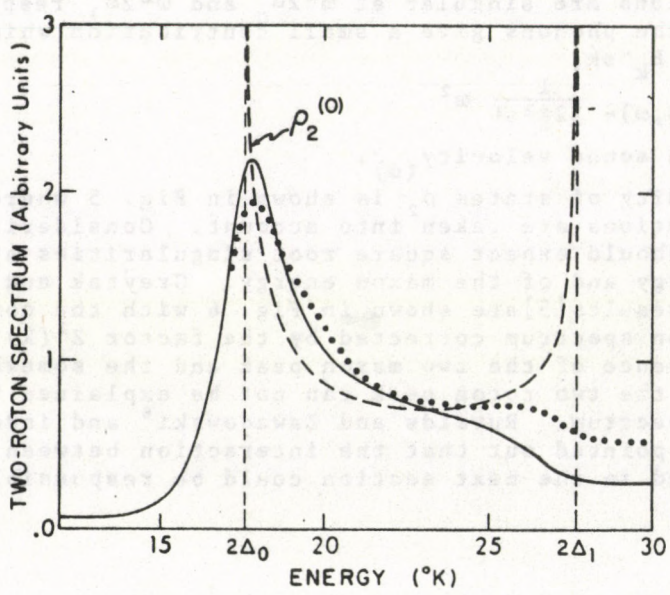

Figure 6. Comparison of theory of non-interacting excitations (dotted curve) with original Raman data of [5].

III. Theory of bound roton pairs

As it has been discussed before, the interaction between the excitations must be included to give account for the profile of the Raman spectrum. Unfortunately, a theory for real He^4 is not available because all of the existing theories are based either on some simplifying Ansatz (like that there is no interaction between the excitations or on an expansion in powers of the density of the density of the liquid) and these approximations break down in the real case. Thus, we have good theoretical background for the single excitations but we are lacking in any theoretical knowledge on the remaining interaction acting between the excitations. Therefore, a theory dealing with that interaction must be a semiphenomenological treatment with more emphasis on the effect of an assumed interaction and with less on a microscopic foundation. This somewhat "sloppy" attitude turns up already at the very beginning in the present formulation. Any theory of He^4 must rely either on the particle representation or on the density fluctuations and depending on that it works with He^4 atom field operators or density operators. The formulas derived with interaction in both ways are very similar which suggests that the structure of the dynamical effects is relatively not sensitive to these details.

Following the work of Zawadowski, Ruvalds and Solana[10] the simplest formulation will be presented here where ψ is the He^4 field operator which is quantized in the usual way as

$$\psi(\vec{r},t) = \frac{1}{(2\pi)^{3/2}} \int d^3\vec{k}\; a_k(t) e^{i\vec{k}\cdot\vec{r}} \quad , \tag{21}$$

a_k is the Bose field annihilation operator and we take the temperature to be zero T=0 where it is possible. Now, it is assumed that the single particle spectrum, e.g. in the Feynman Cohen approximation [18], and the Green's functions are fairly well known so the structure in the Green's function is replaced by a single pole with strength $Z_1(k)$, energy E_k, and with a phenomenological temperature dependent width Γ, thus

$$G_1(k,\omega) = \frac{Z_1(k)}{\omega - E_k + i\frac{\Gamma}{2}} \quad , \tag{22}$$

which is the Fourier transform of the one-particle Green's function $G^{(0)}(x-x')$

$$G_1(k,\omega) = \int d^3\vec{x}\; dt \;\; G_1(\vec{x},t) e^{-i(\vec{k}\cdot\vec{x}-\omega t)} \tag{23}$$

It is well known for superfluid He^4 that the single-particle pole occurs also in the density-density correlation function and that explains why the two different approaches result in such similar expressions.

The interaction between single particle excitations is described in terms of a phenomenological Hamiltonian

$$H_{int} = \frac{1}{2}\frac{1}{(2\pi)^3} \int a_{k_1}^{+} a_{k_2}^{+} \gamma(\vec{k}_1\vec{k}_2\vec{k}_3\vec{k}_4) a_{k_4}\, d\vec{k}_1 d\vec{k}_2 d\vec{k}_3 d\vec{k}_4 \tag{24}$$

where $\gamma(\vec{k}_1\vec{k}_2\vec{k}_3\vec{k}_4) \sim \delta(k_1+k_2-k_3-k_3)\tilde{\gamma}(\vec{k}_1\vec{k}_2\vec{k}_3)$ and a model expression will be used for $\tilde{\gamma}$. The simplest possible model is in which $\tilde{\gamma}$ is a constant. If perturbation theory and diagram techniques are used, the

operators in the interaction Hamiltonian are associated with the Green's function, so for any internal interaction point the combination

$$Z_1^{\frac{1}{2}}(\vec{k}_1)Z_1^{\frac{1}{2}}(\vec{k}_2)\,\tilde{}\,(\vec{k}_1\vec{k}_2\vec{k}_3)Z_1^{\frac{1}{2}}(\vec{k}_3)Z_1^{\frac{1}{2}}(\vec{k}_4) \tag{25}$$

appears which will be replaced by a simple coupling g_4. Thus, the interaction is taken in the form

$$H_{int} = \frac{g_4}{2}\int \psi^+(\vec{x})\psi^+(\vec{x})\psi(\vec{x})\psi(\vec{x})d^3\vec{x} \tag{26}$$

and, respectively, in the Green's function the weight factor $Z_1(k)$ is replaced by unity.

For our purposes the single-and pair-excitation spectra are of importance which are simply related to the Green's functions

$$\rho_1(k,\omega) = -\frac{1}{\pi}\,\mathrm{Im}\,G_1(k,\omega + i\delta) \tag{27}$$

and

$$\rho_2(k,\omega) = -\frac{1}{4\pi}\mathrm{Im}\,G_2(K,\omega + i\delta) \tag{28}$$

respectively, where the two particle Green's function is defined as

$$G_2(x-x') = -i\langle T\left\{\psi^+(x)\psi^+(x)\psi(x')\psi(x')\right\}\rangle \tag{29}$$

where $x \equiv (\vec{x},t)$.

The quantities observed in experiments are always expressed by the density operators. In the weak coupling limit, however, the density and field operator are proportional

$$\rho(x) \sim \sqrt{N_o}\left(\psi(x)+\psi^+(x)\right) + \begin{pmatrix}\text{term of higher}\\ \text{order in } \psi\end{pmatrix}, \tag{30}$$

where N_o denotes the number of the particles in the Bose condensate with zero momentum. On the other hand, using the quasiparticle picture the density is expressed by the quasiparticle operators in a similar way

$$\rho_k \sim \left(\alpha_k^+ + \alpha_{k-}\right) + \text{(terms of higher order)} . \tag{31}$$

On the basis of this similarity it is assumed that the Raman scattering is related to the following correlation function

$$\langle a_k^+(t)\, a_{-k}^+(t)\, a_{k'}(0)\, a_{-k'}(0)\rangle \tag{32}$$

which has a close connection to the quantity discussed previously and given by (12).

If two rotons are excited by light or neutrons and similar excitations are thermally not excited, only these two excited rotons can interact by the roton-roton interaction. Therefore, this problem can be regarded as a two body problem and the interaction can be taken into account by the Bethe-Salpeter equation or by the ladder diagrams, in other words. The bubble diagrams to be summed up are depicted in Fig. 7 and the corresponding equation for the Green's function is

$$G_2(x-x') = 2i\left[\left(G_1^{(0)}(x-x')\right)^2 + 2ig_4\int d^4x''\left(G_1^{(0)}(x-x'')\right)^2\left(G_1^{(0)}(x''-x')\right)^2 + \right] . \qquad (33)$$

Figure 7. Diagrammatic representation of the multiple scattering of two rotons.

The Fourier transform of the contribution of the simple loop diagram $F(x-x')=i\left[G_1^{(0)}(x-x')\right]^2$ with total momentum and energy K and ω respectively, is

$$F(K,\omega) = \frac{1}{i(2\pi)^4}\int d^3\vec{k}'\,d\tilde{\omega}\; G_1^{(0)}(k',\tilde{\omega})G_1^{(0)}(k-k',\omega-\tilde{\omega}) \quad , \qquad (34)$$

and by using this notation the sum of the series discussed above can easily be obtained as

$$G_2(K,\omega) = \frac{2F(K,\omega)}{1-g_4F(K,\omega)} \qquad (35)$$

By inserting this result into (28) one gets the two particle density of states

$$\rho_2(k,\omega) = -\frac{1}{4\pi}\,\mathrm{Im}\,G_2(K,\omega) = -\frac{1}{2\pi}\frac{\mathrm{Im}\,F(K,\omega)}{\left[1-g_4\,\mathrm{Re}F(K,\omega)\right]^2+\left[g_4\,\mathrm{Im}F(K,\omega)\right]^2} . \qquad (36)$$

Finally, it is useful to give the spectral representation of the function $F(K,\omega)$ which is derived by calculating the integrals on the right hand side of (34) using the notation given by (4) and it is

$$F(K,\omega) = 2\int \frac{\rho_2^{(0)}(k,\omega')}{\omega-\omega'+i\Gamma}\,d\omega' \quad . \qquad (37)$$

Thus knowing the density of states for two noninteracting particles with infinite lifetime the renormalized two-particle density of states and Green's function can be calculated by using (34), (35), and (37). In the following $\rho_2(k,\omega)$ will be calculated in two different cases as K=0 and $K\neq 0$ ($K \sim k_0$). Formation of a bound state can be expected if Γ is taken to be zero ($\Gamma=0$) and if the decay of two rotons or two maxons into the two phonon continuum is ignored. Otherwise the poles in G_2 may refer to possible resonances.

Bound state with K=0.

The experimentally observed Raman spectrum is shifted in the direction of lower energies compared to the noninteracting case as it

is shown in Fig. 6 and that indicates that the interaction is attractive. For the sake of simplicity the calculation to be carried out is restricted to the region of energy $\omega \sim 2\Delta_0$. Inserting $\rho_2^{(0)}(K,\omega)$ from (20a) into (37) and performing the integral one finds for $\Gamma=0$ and $E=\omega-2\Delta_0<0$ that

$$F(K=0,E>0)=-4\left(\frac{k_0}{2\pi}\right)^2\mu_0^{\frac{1}{2}}\left[\tan^{-1}\left|\frac{2D}{E}\right|-i\delta\right]|E|^{-\frac{1}{2}} \quad , \qquad (38)$$

and for $E>0$,

$$F(K=0,E>0)=2\left(\frac{k_0}{2\pi}\right)^2\mu_0^{\frac{1}{2}}E^{-\frac{1}{2}}\left(\ln\left|\frac{E^{\frac{1}{2}}+(2D)^{\frac{1}{2}}}{E^{\frac{1}{2}}-(2D)^{\frac{1}{2}}}\right|-i\pi\right) \quad , \qquad (38)$$

where D is the cut-off energy used in the momentum integral. Considering the region $E<0$, this gives $\mathrm{Im}F=0$ and so according to (36) one gets

$$\rho_2(K=0,E<0)=\frac{1}{2|g_4|}\,\delta\left(1-g_4\,\mathrm{Re}F(K=0,E<0)\right) \quad . \qquad (39)$$

Thus one finds a bound state at that energy $E=E_B$ where $g_4\,\mathrm{Re}F\big|_{E=E_B}=1$. In the weak coupling limit $\tan^{-1}\left|\frac{2D}{E}\right|\sim\frac{\pi}{2}$,

hence

$$E_B=-\pi^2 2D(\hat{g}_4)^2 \quad , \qquad (40a)$$

and

$$\rho_2(K=0,E)=\tfrac{1}{2}\eta\,|\hat{g}_4|^2\pi\delta\left(\frac{E-E_B}{2\Delta_0}\right) \quad , \qquad (40b)$$

whre $\hat{g}_4=\tfrac{1}{2}g_4 k_0^2\,\frac{1}{\pi^2}\left(\frac{\mu_0}{2D}\right)^{\frac{1}{2}}$ is the dimensionless coupling.

Thus a bound state occurs in the case of an arbitrary weak attractive interaction, but its strength in ρ_2 goes to zero as $g_4\to 0$. In Fig. 8 the result of a more complete calculation is shown, where the unperturbed density of state in the region $2\Delta_0<\omega<2\Delta_1$ is the sum of expressions (20a) and (20b) corresponding to the rotons and maxons, as well, and $\rho_2^{(0)}=0$ otherwise. Furthermore, the effect of a single roton linewidth is illustrated in Fig. 9 in which case resonances are formed instead of bound states. The density of states obtained has a strong resemblance with the Raman spectrum shown in Fig. 6.

It has already been discussed in section II that by optical experiments only the d-like pair excitations are observed. Thus in order to extend the calculation to states with arbitrary symmetry the interaction given by (26) must be generalized for total momentum $K=0$ as

$$H_1=\frac{1}{4}\sum_{kk'}V_{kk'}a_k^+\,\underline{a}_k^+\,a_{k'}\,\underline{a}_{k'} \qquad (41)$$

where the general interaction potential $v_{kk'}$ can be expanded in terms of spherical functions

$$V_{\vec{k}\vec{k}'} = \sum_{\ell}(2\ell+1) g_4^{\ell} P_{\ell}(\cos\Theta_{kk'}) = \sum_{\ell} g_4^{\ell} \sum_{m} 4\pi \left(Y_{\ell}^{m}(\vec{K})\right) Y_{\ell}^{m}(\vec{K}') \qquad (42)$$

where g_4^1 is the coupling in channel 1, and the function F must be also generalized as

$$F_{\ell m} = \frac{1}{(2\pi)^3} \int d^3\vec{k}\, d\omega\, Y_{\ell}^{m}(k) \left(Y_{\ell}^{m}(k')\right)^{*} G_1(k,\tilde{\omega}) G_1(-k, \omega-\tilde{\omega}) \qquad (43)$$

and then the density of states in the channel of the quantum numbers ℓ and m is

$$\rho_{2\ell}^{m} = \frac{1}{4\pi} \operatorname{Im} \frac{F_{\ell m}}{1 - g_4^{\ell} F_{\ell m}} \qquad . \qquad (44)$$

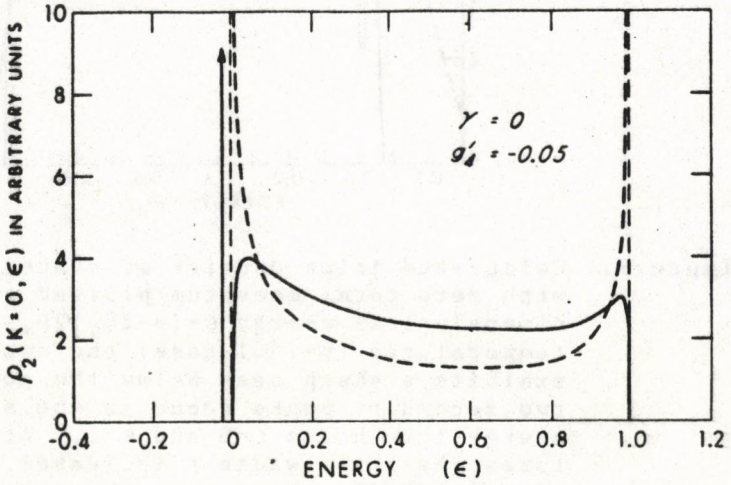

Figure 8. Calculated joint density of states ρ_2 for two rotons with zero total momentum plotted as a function of dimensionless energy $E=(\omega-2\Delta_0)/2D$. Dotted lines indicate the spectrum in the absence of interactions. Inclusion of an attractive roton-roton coupling removes the singularities at E = 0 and E = 1, shifts the spectrum to lower energies, and splits a two-roton bound state off below the two-roton continuum as shown by the solid lines. In this figure the single roton lifetime was taken to be infinite, i.e. $\delta=\Gamma/\Delta=0$ and $g_4^1 = g_4 \frac{1}{2} k_0^2 \pi^{-2} (\mu_0/2D)^{\frac{1}{2}}$ is the dimensionless coupling.

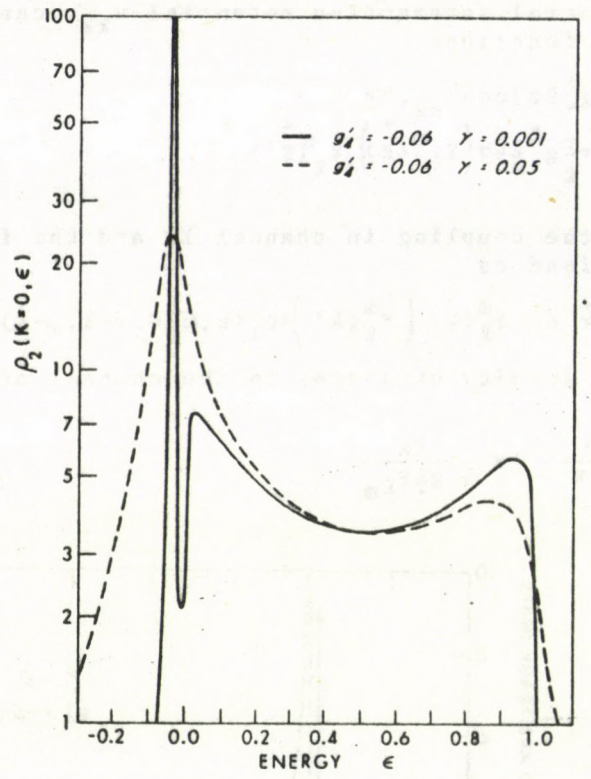

Figure 9. Calculated joint density of states ρ_2 for two rotons with zero total momentum plotted as a function of dimensionless energy $\varepsilon=(\omega-2\Delta_0)/2D$, and $\gamma=\Gamma/\Delta_0$. At low temperatures ($\gamma=.001$ case) the two-roton bound state exhibits a sharp peak below the continuum ($\varepsilon<0$) while two secondary peaks occur in the spectrum near the energy thresholds $\varepsilon=0$ and $\varepsilon=1$. At higher temperatures the roton width γ increases and, as in the example $\gamma=.05$, smears out the secondary peak structure. In the latter case the spectrum is dominated by a single peak near $\varepsilon=0$ in accord with experiment. [$g_4^1=g_4 \tfrac{1}{2} k_0 '\pi' (\mu_0/2D)^{\frac{1}{2}}$.]

In this limit K=0, however, the function F_{lm} and the coupling must be independent of m because of the rotational invariance. Furthermore, l must be even number, because the wave function of Bose particles is symmetric in the variables. Thus if g_4^l l=0,2,4... is negative a bound state is formed and in this way a series of different bound states may exist, which are degenerate regarding the quantum number m. But, if the total momentum K is not zero and then choosing the rotational axis parallel to K the bound state for a given l with K=0 splits for different m. This situation is illustrated in Fig. 10 and it is discussed by Pitaevskij and Fomin [19] in detail. As any satisfactory microscopic model for the roton-roton interaction has not been proposed yet, the question that in which angular momentum channel is the interaction attractive is completely open, except that the light scattering experiment gives direct evidence for the bound state in the channel l=2 thus $g_4^{l=2}<0$.

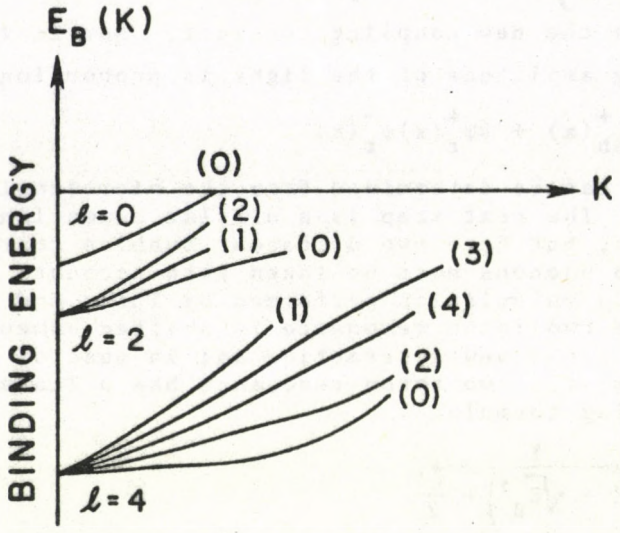

Figure 10. A schematic plot of the momentum dependence of possible two-roton resonances with different quantum numbers; various helicity values are indicated by (m).

As it is discussed by Greytak in this school the theory presented here describes the two-roton state with great accuracy regarding the anomalous lineshape and the binding energy as well. The new neutron scattering data [20] for the roton energy is extremely accurate and agrees very well with that determined from the profile analysis of the Raman spectrum [21] where the roton energy was an adjustable parameter. These new results rule out any doubt about that the roton-roton interaction is negative in channel l=2.

There is, however, one theoretical question left, namely, the linewidth of the single roton at very low temperature.

As the single roton can not decay, because the energy and momentum conservation can not be satisfied simultaneously, thus the single roton linewidth must be zero at T=0. From the Raman experiments the parameter Γ is determined by fitting and this procedure provides a temperature dependence for Γ which agrees very well with other data for the single roton linewidth at high temperature, but it definitely shows that this fitting parameter does not go to zero as the zero temperature is approached. This discrepancy can be solved by the proposition of Iwamoto [7], Greytak [21], Jackle and Beareswyl [22, 13], Pitaevskij, Fomin [19] and recently of Tutto that the decay of the two-roton state into the continuum of the two-phonons must be taken into account.

The theory adequate to describe this phenomenon is very simple and its formulation is based on the introduction of two different fields as the roton and phonon fields ψ_r and ψ_{ph} which are defined by (21) where the momentum integrals are restricted to the appropriate regions. The model Hamiltonian given by (26) must be completed by another term H_{2ph} which is

$$H_{r-ph}=g_{r-ph}\int\psi_r^+(x)\psi_r^+(x)\psi_{ph}(x)\psi_{ph}(x)d^3x + c.c. \qquad (45)$$

where g_{r-ph} is the new coupling constant. Now it is assumed that the scattering amplitude of the light is proportional to

$$A\psi_{ph}^+(x)\psi_{ph}^+(x) + B\psi_r^+(x)\psi_r^+(x) \quad , \qquad (46)$$

where A and B can be determined from the microscopic theory of Stephen [12]. The next step is a similar summation of bubble diagrams as before, but here two different bubbles corresponding to two rotons and two phonons must be taken into account. The rather straightforward calculation performed by Tüttő and Zawadowski [23] * shows that the two-roton resonance is shifted somewhat to larger energies due to the new interaction and in case of rotons with infinite lifetime the two roton resonance has a lineshape determined by the following formula

$$L(E)\simeq \frac{1}{\left(\sqrt{E}-\sqrt{E_B}^2\right)+\frac{\Gamma'}{2}} \qquad (47)$$

where E is measured from the two roton energy $2\Delta_0$, E_B is the renormalized binding energy and Γ' is a new parameter which is finite. The two new parameters E_B and Γ' are determined by the coupling g_{r-ph}, the speed of sound s and the ratio A/B for what $A/B \ll 1$ holds. Finally, in the limit $A/B \sim 0$ there is only one unknown parameter g_{r-ph}.

This parameter was estimated by Tüttő [24] considering the two phonon-two roton vertex which is assumed to have the internal structure shown in Fig. 11 where the two-phonon process is decomposed into two one-phonon processes. This diagram contains the roton-phonon vertex which is known at least in the long wave length limit in the deformation potential approach where that is proportional to the derivative of the roton energy with respect to the density of the liquid $\partial\Delta/\partial\rho$. This quantity is known from the experiments in which the pressure dependence of the roton energy has been measured by neutron scattering [25]. The other vertex is connected to two roton lines going in one direction and to a phonon line. In the weak coupling limit it can be shown [26] that this latter vertex is related to the previous one by a numerical factor 2. Accepting this relation between the vertices the vertex in Fig. 11 can be estimated in the long wave length limit and according to Tüttő [24] the value obtained explains the finite value of Γ found experimentally for $T \to 0$. Finally, the experimental confirmation of the $\sqrt{E}$ dependence in the lineshape proposed by this theory and given by formula (47) should be the target for further experiments.

* See the original work by R. L. Woerner and M. J. Stephen J. Phys. C. 8 L 464 (1978).

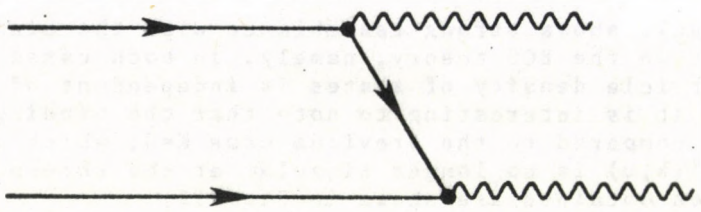

Figure 11. The coupling of two phonons with a roton pair (dotted Lines). The vertices are the usual phonon-roton interactions.

Bound States With K≠0

As it has already been indicated in Fig. 10, a bound state at K=0 can be the end point of a bound state dispersion curve which extends for larger momentum region. There is, however, no experiment which could give direct information on the two roton states with larger total momenta. The neutron scattering cross section with energies $\omega > 2\Delta_0$ (upper branch of the spectrum) is in strong connection with the roton pairs as will be discussed in section V., furthermore, the energy dependences of the roton energy and lifetime give some indirect but very firm information.

First, let us consider a Hamiltonian which is without any structure; thus it is given by (26). The two-roton density of states can be calculated from the unrenormalized one. For larger momenta ($k \sim k_0$), $\rho_2^{(0)}(K,E)$ is energy independent above the threshold energy $2\Delta_0$ and it shows 1/K dependence as

$$\rho_2^{(0)}(K\neq 0,\omega)=\rho_0(K)=\frac{1}{K}\,\frac{\mu_0 k_0^2}{4\pi}\ , \quad \text{for } K>2k_0 \tag{48}$$

This result is obtained by an elementary calculation using (4) and (20a). The interpolation formula between the two simple results (20a) and (48) has a rather complicated algebraic form and we refer to the Appendix of [10]. Using this result above the F function defined by (37) can be calculated in a simple way and one gets

$$\mathrm{Re}F(K,\omega)=\rho_0(K)\ln\frac{E^2+\Gamma^2}{4D^2}\ , \tag{49}$$

and

$$\mathrm{Im}\,F(K,\omega)=2\rho_0(K)\left[\frac{1}{2}\pi+\tan^{-1}\frac{E}{\Gamma}\right]\ , \tag{50}$$

for $E \ll D$, where D is the cut-off parameter.

An analysis similar to the case K=0 gives a bound state for arbitrary small coupling strength, if $g_4<0$ and $\Gamma=0$, thus

$$\rho_2(K,\omega)=\frac{1}{2|g_4|}\,\delta\left(1-2g_4\rho_0(K)\ln\frac{E}{2D}\right)\ , \tag{51}$$

and the binding energy E_B is

$$E_B = 2D\exp\left\{-1/\left(2g_4\rho_0(k)\right)\right\} \qquad (52)$$

This result shows strong resemblance with the binding energy of a Cooper pair in the BCS theory, namely, in both cases the unrenormalized two-particle density of states is independent of the energy. Furthermore, it is interesting to note that the binding energy is rather small compared to the previous case K=0, which is due to the fact that $\rho_2^0(k,\omega)$ is no longer singular at the threshold $\omega=2\Delta_0$. The lineshapes obtained are shown in Fig. 12.

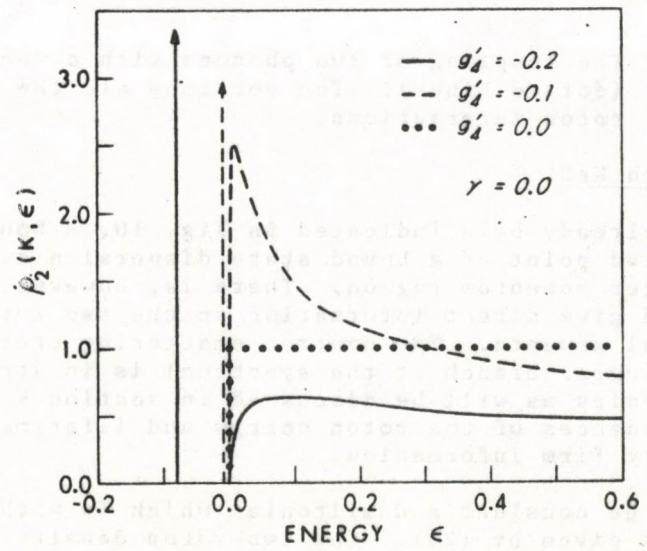

Figure 12. Calculated two-roton spectrum ρ_2 at finite total momentum including a finite single roton width γ. The dimensionless energy is $\epsilon=(\omega-2\Delta_0)/2D$, and $\gamma=\Gamma/\Delta_0$. The dotted curve gives the unperturbed density of states, while the dashed and solid lines display the spectrum including interactions for $\gamma=.02$ and $\gamma=.05$ respectively. As a consequence of the attractive roton-roton coupling $g_4' g_4 \frac{1}{2} k_0' \pi^{-2} (\mu_0/2D)^{\frac{1}{2}}$, the spectrum exhibits a sharp peak near the two-roton energy threshold ($\epsilon = 0$).

The symmetry considerations on the bound state will play an important role in the further discussions, therefore, the general results of Pitaevskij and Fomin [19] will be briefly discussed. They assumed a roton-roton interaction which depends only on angle determined by the change in their directions and they proved in this way, that the dispersion curves of the bound states have their minima at K=0. At larger K the energy of the l-bound state (l=0,2,4, ...) which is (21 + 1) - fold degenerate, splits according to the absolute value of the "helicity" quantum number ℓ. By increasing K further the binding energy very likely decreases as in the simplest case it is demonstrated by the expressions (40) and (52) valid for K=0 and K≠0, respectively. It is obvious, that two dispersion curves starting from two different bound states at K=0, but with the same helicity m can not intersect. Thus, either these curves end at the threshold energy $2\Delta_0$, but at different momenta, or they approach continually

that energy. At larger momenta, however, the situation is essentially simplified. In the momentum space the rotons are near the sphere with radius k_0. Keeping the total momentum K of the pair fixed the rotons can be found in the neighborhood of a spherical zone with solid angle $2\arccos(K/K_0)$. In this case, the roton-pair is determined by the total energy E_k+E_{K-k} and by the plane of the momenta, which plane is characterized e.g. by the angle Θ shown in Fig. 13 (Θ is the angle between that plane and the x-axis if the y-axis is chosen to be parallel to K). In order to have a symmetric pair wave function with large enough K the helicity must be even m=0,2,4, ... , but this does not hold for small K≈0. Furthermore, if the bare vertex is smooth as a function of the energy of the pair $E_k + E_{K-k}$ for fixed K, not more than one bound state can be expected for a given m. Thus, either all of the bound state dispersion curves end with small momenta at the threshold energy $2\Delta_0$ of the continuum or only the one belonging to the lowest lying bound state at K=0 approaches the threshold in a large range of momenta and finally that may or may not end. According to the previous discussion that surviving bound state may exist only for even m.

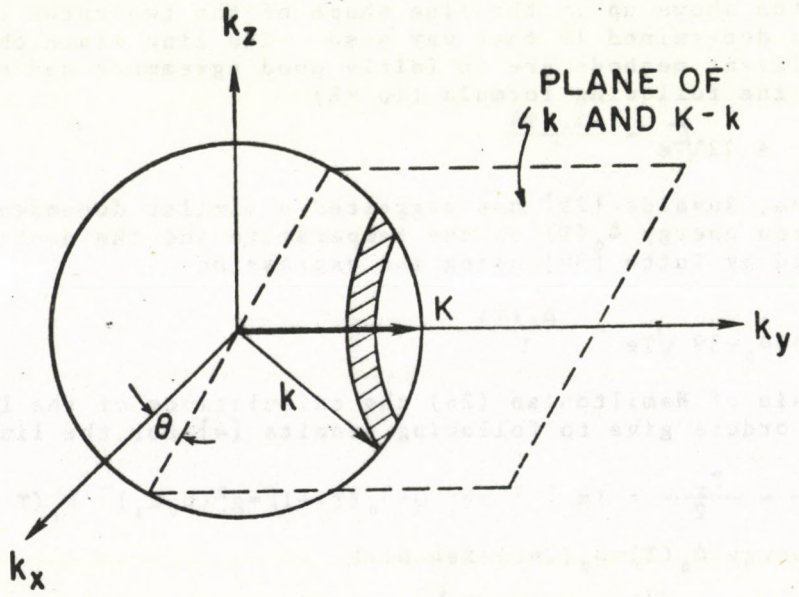

Figure 13. The roton sphere is shown with radius k_0 in momentum space. The momentum of a roton pair with momenta k and K-k forms a plane which is characterized by an angle Θ. The pair total momentum K is near the spherical zone indicated by latched area.

The Hamiltonian H_k describing the interaction of roton pairs with K can be given as

$$H_K=\sum_{kk'} g_4^{(m)}(K)\, e^{im(\Theta-\Theta')}\, a_{k'}^{+} a_{K-k'}^{+} a_k a_{K-k} \quad , \qquad (53)$$

where the coupling constant $g_4^m(K)$ is expanded in a Fourier series as a function of the angle $\Theta-\Theta'$, between the planes of the momenta before and after the scattering and in the coefficients $g_4^{(m)}(K)$:

the dependence on k and k' is neglected. In the case of $g_4^{(m)}(K)<0$ with m=0,2,4, ... a bound state exists with binding energy

$$E_B^{(m)}=2D\exp\left\{-1/(2g_4^{(m)}(K)\rho_0(K)\right\} \quad . \qquad (54)$$

Finally it may be mentioned that in the region $K>2k_0$ in the threshold of the continuum bends in the upper direction, thus the dispersion curve of an existing bound state must turn upward, as well.

IV. Temperature Dependence of the Roton Lifetime and Energy

The roton-roton interaction shows up in the temperature dependence of the single roton energy and lifetime if many body corrections are calculated. It was first suggested by Landau and Khalatnikov [4] that the lifetime τ_r in the temperature range 1.2 - 1.8°K is dominated by the roton-roton scattering process in which a single roton is knocked by a thermally excited one, thus $1/\tau_r \sim N_r(T)$. This conclusion was first drawn from the viscosity data, see [27]. Later it was confirmed by neutron scattering measurements of line width of a single roton excitation [25]. Furthermore, as we have already discussed in the previous section, the line width Γ_r of a single roton shows up in the line shape of the two-roton resonance and Γ_r was determined in that way also. The line width obtained by these different methods are in fairly good agreement and they can be fitted by the following formula (in °K)

$$\frac{\Gamma_r}{2} = 42\sqrt{T}e^{-\frac{\Delta_0(T)}{T}} \quad . \qquad (55)$$

Furthermore, Ruvalds [29] has suggested a similar dependence of the single roton energy $\Delta_0(T)$ on the temperature and the neutron data were fitted by Tutto [30] using the expression

$$\Delta_0(T)=\Delta_0-39\sqrt{T}e^{-\frac{\Delta_0(T)}{T}} \quad . \qquad (56)$$

On the basis of Hamiltonian (26) the calculations of the lowest non-vanishing orders give to following results [4] for the line width

$$\frac{1}{\tau_4}=\frac{\Gamma_r}{2}=\mathrm{Im}\,\Sigma\left(k=k_0,\omega=\Delta_0(T)+T\right)=g_4^2(\mu_0 k_0)^{-1}N_r(T) \quad , \qquad (57)$$

and the energy $\Delta_0(T)=\Delta_0(T=0)+\mathrm{Re}\Sigma$ with

$$\mathrm{Re}\Sigma\left(k=k_0,\omega=\Delta_0(T)\right)=2g_4N_r(T) \qquad (58)$$

where simply the golden rule and the Hartree Fock term [29] have been evaluated. The common nature of both expressions are that by fitting the experimental data such values are obtained for the coupling constant $g_4=-3.7\ 10^{-38}$ erg cm^3 and $g_4=2.4\ 10^{-38}$ erg cm^3 which are in an order of magnitude larger than the estimate based on the two roton resonance $g_4^{l=2}=-1.2\ 10^{-39}$ erg cm^3. This contradiction is not very serious itself, because the couplings can be very different in different ranges of the momenta K and in the different channels. Considering the lifetime the most important energy region is $3/2k_0 < K < 2k_0$ [30, 31] in contrast to the bound state at K=0. The main objection is, however, that these values of the coupling are actually so strong that the restriction to the lowest orders of the perturbation theory is incorrect.

In the following the theory with structureless coupling will be discussed and it will be shown that the experimental facts can not be explained in that way, therefore, finally the structure in the coupling is considered.

The temperature region of interest is where the real and imaginary parts of the self-energy are proportional to the number of the rotons $N_4(T)$ in thermal equilibrium. Thus, those time ordered diagrams must be considered where there is only one backward running roton line. These diagrams are of the type shown in Fig. 14. These processes have been considered by Yau and Stephens[32], Nagai, Nojima, Hatano[21], Fomin[33] and Solana, Celli, Ruvalds, Tutto, Zawadowski[33] and Kebuwa[36] for the energy shift.

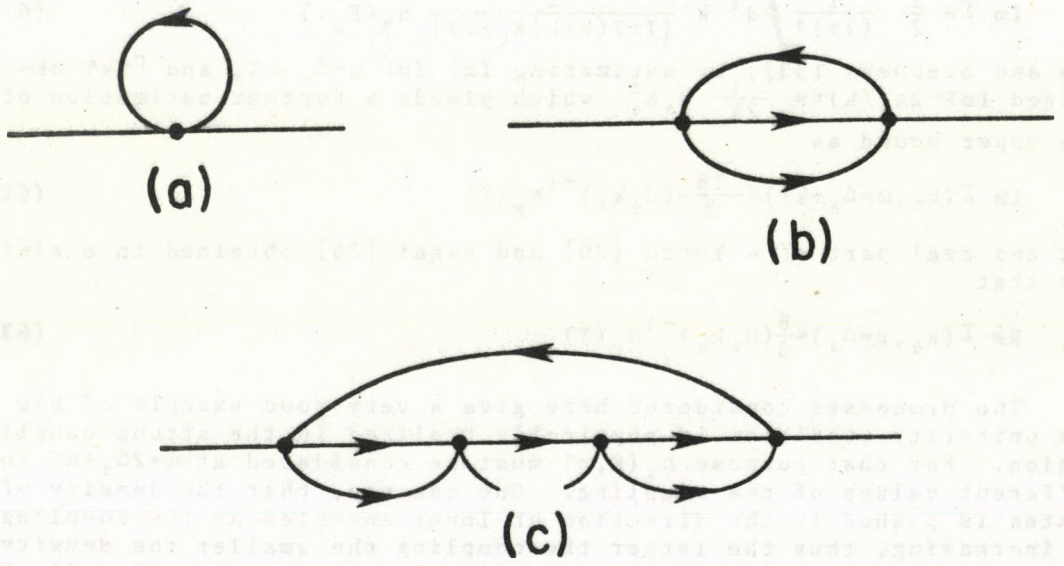

Figure 14. The time ordered diagrams contributing to the self energy and lifetime of rotons. (a) Hartree-Fock term (b) leading order contribution to the lifetime (c) general higher-order diagram with one backward roton line.

In the temperature dependent Green's function technique the contribution of these diagrams is

$$\Sigma(k,i\omega_n) = -T\sum_n' \int \frac{d^3k}{(2\pi)^3} G_1(K,i\omega_n') \left\{ 2g_4 + g_4^2 G_2(K=k, i\omega_n + i\omega_n') \right\} , \qquad (59)$$

with $\omega_n = 2\pi nT$, where the first term is the Hartree-Fock one. Making use of the spectral representations given by (27) and (28) and the expression (35) this equation can be written in the form

$$\Sigma(k,\omega) = \int \frac{d^3k}{(2\pi)^3} \int d\tilde{\omega}\, n_B(\tilde{\omega})\rho_1(k,\tilde{\omega}) \frac{2g_4}{1-g_4 F(K+k, \omega+\tilde{\omega})} , \qquad (60)$$

which formula reproduces the previous results given by (57) and (58) in the weak coupling limit. On the other hand, it is interesting to note that the real imaginary parts of the self energy go to a finite limit as $g_4 \to \infty$. It must be so, because, any scattering process has an upper bound called the unitarity limit, because only a part of the incident particles can be scattered regardless of the strength of the bare interaction.

In order to discuss first the imaginary part by using (36) we transform that into another form which can be interpreted according to the golden rule. Thus a roton with energy $\tilde{\omega}$ and momentum k' is thermally excited which hits another roton and $\rho_2(K,\omega+\tilde{\omega})$ is the density of the states in the final state where the final state interaction is also included. Using the approximation and (35), an upper bound is

$$\text{Im}\ \Sigma = \frac{1}{2}\ \frac{1}{(2\pi)^3}\int d^3k' \frac{1}{|\text{Im}F(k+k';E_{k'}+\omega)|}\ n_B(E_{k'}) \qquad (61)$$

Yau and Stephens [33], by estimating ImF for $\omega=\Delta_0+kT$, and $\Gamma \ll kT$ obtained $\text{Im}F \sim 2\rho_0(K)\pi = \frac{1}{2K}\ \mu_0 k_0^2$ which yields a further estimation of the upper bound as

$$\text{Im}\ \Sigma(k_0,\omega=\Delta_0+kT) < \frac{16}{3}(\mu_0 k_0)^{-1} N_r(T) \qquad (62)$$

For the real part of Σ Tutto [30] and Nagai [36] obtained in a similar way that

$$\text{Re}\ \Sigma(k_0,\omega=\Delta_0) < \frac{8}{3}(\mu_0 k_0)^{-1} N_r(T) \qquad (63)$$

The processes considered here give a very good example of how the unitarity condition is physically realized in the strong coupling region. For that purpose $\rho_2(K,\omega)$ must be considered at $\omega=2\Delta_0+kT$ for different values of the coupling. One can see, that the density of states is pushed in the direction of lower energies as the coupling is increasing, thus the larger the coupling the smaller the density of states is just above the energy $2\Delta_0$. In this way $g_4\rho_2(K,\omega=2\Delta_0+kT)$ remains finite.

The real and the imaginary parts of the self energy are shown as the function of the coupling in Fig. 15. First of all these results clearly show how the approximations of the lowest order given by (57) and (58) break down with increasing coupling. As the temperature dependent correction to the roton energy is negative g_4 must be negative and it can not exceed a critical value about 1.5×10^{-38} erg cm^3, because Re Σ changes sign there. A simple estimation shows that the upper bound for the inverse theoretical lifetime is 1/4 of the experimental one and for the energy shift this ratio is even smaller 1/6. These most favorable values of the coupling are different, thus with one single value of the coupling that ratio is even smaller, less than 1/7. The conclusion drawn is very definite and it states that a simple structureless coupling can not explain more than about 1/7 of the experimental values which is obtained with a g_4 a little bit smaller than -1.0×10^{-38} erg cm^3.

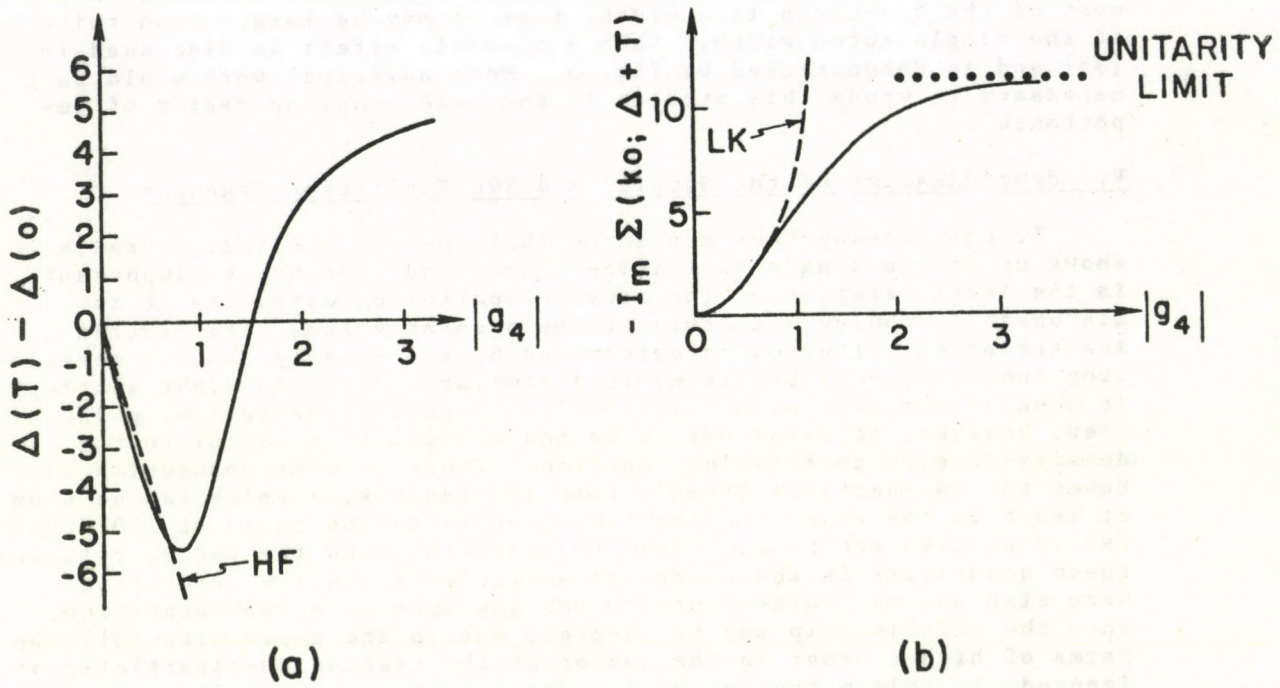

Figure 15. (a) Energy shift of the roton $\Delta(T)-\Delta_0$ in units of $T^{\frac{1}{2}} \exp(-\Delta/T)$ at $T=1.2^0$k, as a function of the coupling. The dashed line shows the Hartree-Fock approximation. (b) Imaginary part of the roton self energy in units of $T^{\frac{1}{2}} \exp(-\Delta/T)$ at $T=1.2^0$k. The unitarity limit is shown by the dashed line, whereas the Born approximation gives the dotted curve.

It has been pointed out by Fomin[34] that a more complicated coupling contained by the Hamiltonian (53) may help to resolve that disagreement. Namely, the channels with different helicity m are completely decoupled, thus the contributions to Im Σ from the different channels are additive. That means that at least in seven channel e.g. in the channels $m=0,\pm2,\pm4,\pm6$, or more the couplings with the most favourable values are necessary to explain the experimental data considered here. Thus, at least in seven channels the coupling must be attractive in the most effective energy range $3/2K_0<K<2K_0$. Apparently, this means that at K=0 there must be at least one or two more bound states additional to the one with l=2 and at least for one of these l>4 must hold. Furthermore, it is obvious that this consideration does not contain any piece of information whether the bound state with l=0 exists or not, which is crucial for the neutron scattering to be discussed in the next section.

The last remark to be made is about the line width extracted from the line shape of the two roton resonance measured by Raman scattering. In these experiments the thermally excited roton knocks

the two roton resonance, thus the total energy of the system is about $3\Delta_0 - E_B + kT$. Thus, two rotons in the final state may form also a resonance and in this way their energy may be below $2\Delta_0$. In this region, however, the two-roton density of states may result in an enhencement of the two-roton line width, thus it may be larger than twice of the single-roton width. Such a possible effect is discussed in [35] and is demonstrated by Fig. 6. More numerical work would be necessary to study this problem in the weak coupling region of importance.

V. Hybridization of the Single- and Two-Excitation Branches

It has already been mentioned that the two-excitation branch shows up in the single excitation branch and that may be important in the interpretation of the neutron scattering data. As it is discussed in Cowley's lecture of the present volume, the neutron scattering distribution is determined by the density-density correlation function, thus by $S(k,\omega)$ in a similar way to the light scattering in case of the mechanism (i) see (8). From the theoretical point of view, however, it turns out to be too difficult to calculate the density-density correlation function. There is some connection between the one-particle Green's function and $S(k,\omega)$ which can be seen at least in the weak coupling limit, where on the basis of (30) these two quantities are proportional to each other and the factor relating these quantities is the number of particles N_0 in the condensate. Here also one may rather turn to the quasiparticle representation, then the relationship may be clearer, but in the expression (31) the terms of higher order in the number of the created quasiparticles are ignored, in this method as well. The formalisms are different in these two cases, but the results obtained show very similar behavior again.

As we do not have clear reliable theoretical predictions on the one-excitation two-excitation vertex, we should start with a phenomenological Hamiltonian

$$H_3 = g_3 \int \psi^+(x)\psi^+(x)\psi(x)d^3x + \text{c.c.} \qquad (64)$$

where $g_3(K)$ is the coupling.

A similar Hamiltonian has been used by Pitaevskij [2]. The treatment presented here will closely follow the work of Zawadowski, Ruvalds and Solana [8,10] which has many similarities with that of Iwamoto [38].

The basic framework of our formulation is the following. The main features of the Feynman Cohen theory [18] for the single excitation branch is accepted which can be regarded as the single-particle branch as well. As it is shown in Fig. 2 this branch goes through the two-excitation continuum which consists first of all of rotons and maxons. The branches of more than two excitations are beyond the scope of the present treatment. The Hamiltonian introduced here describes an interaction between the single-and two-particle branches, where the latter one has a lower threshold at energy $2\Delta_0$. As in all of the similar cases a hybridization of these two branches occurs, which results in two nonintersecting branches with some kind of level repulsion. The bending of the lower branch shown in Fig. 2 and first suggested by Pitaevskij [2] is certainly a hybridization effect. Then the lower branch formed has a single particle character at lower momenta and continuously as it approaches the threshold of the

continuum it looses the single-particle feature by becoming a two-roton excitation. On the other hand at lower momenta the two-roton excitation branch around or above $2\Delta_0$ bends upward as getting nearer to the single excitation branch and continuously goes into that at higher energies. In the following treatment we put more emphasis on the energy region above $2\Delta_0$ and by that we complete Pitaevskij's original work [2]

Before starting with the detailed calculation it must be pointed out that a single-excitation, which in the momentum space is invariant with respect to its momentum as rotational axis, can interact with the two-excitation continuum of the same symmetry, thus, of helicity m=0. In this way the states with helicity $m\neq 0$ are irrevelant in this problem, so $g_4(K)$ means $g_4^{m=0}(K)$ in the following.

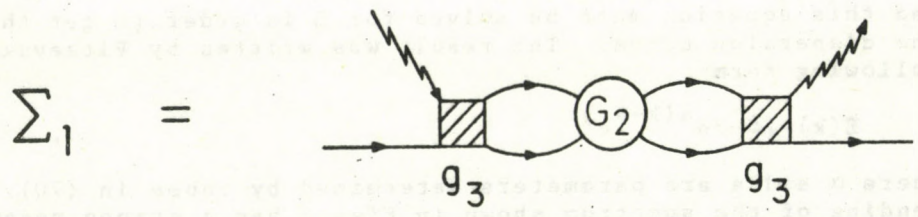

Figure 16. Dyson equation for the single particle self energy Σ_1. The propagator G_2 includes bound roton pairs and is shown in Fig. 7. The zig-zag lines represent particles from the condensate and the hybridization coupling is $g_3=g_4[N_0(T)]^{\frac{1}{2}}$, where $N_0(T)$ is the number of particles in the condensate.

The hybridization process due to the Hamiltonian given by (64) can be described by the diagrams in Fig. 16 where the effect of the couplings g_3 and g_4 are considered as well. In the mathematical form these processes result in a self energy of the one-particle Green's function as

$$\Sigma_1 = 2g_3^2 \frac{F(k,E)}{1-g_4F(k,E)} \quad , \tag{65}$$

where the form (35) of the two-particle Green's function with $g_3=0$ has been used. Thus, the one-particle Green's function for $E<0$ and $\Gamma=0$ has the form

$$G_1^{-1}(k,E<0)=E-E_k-g_3^2(k)\frac{4\ell n\frac{|E|}{2D}}{1-2g_4(k)\rho_0(k)\ell n\frac{|E|}{2D}} \quad , \tag{66}$$

where $E=\omega-2\Delta_0$.

Let us start with the discussion of the region $E<0$. Without hybridization the two-roton continuum has no contribution to this region if $g_4>0$ and only the two-roton bound state contributes if $g_4<0$. In the first case the expression (66) can be rewritten as

$$G^{-1}(k,E)=E-E_k+\frac{g_3^2(k)}{g_4(k)\rho_0(k)}-2\frac{g_3^2(k)}{g_4(k)\rho_0(k)}\frac{1}{1+2g_4(k)\rho_0(k)\ell n\frac{|E|}{2D}} \quad . \tag{67}$$

It can be seen that the effect of the continuum is small as far as ω is far from the energy $2\Delta_0$ and the contribution of the last term on the right hand side of (67) is independent of the energy. As $E \to 0$, the last term, however, starts to decrease and that results in the bending of the spectrum determined as a pole in the Green's function. As it has been pointed out by Pitaevskij [2] in case of $E=0$ the last term vanishes, and the momentum value k_c where the single-excitation branch reaches the continuum is determined as

$$E_c = 2 \frac{g_3^2(k)}{g_4(k)\rho_0(k)} \quad , \tag{68}$$

where $E_c = E(k)\big|_{k=k_c}$. Near the threshold the behavior can be obtained easily by subtracting (67) from (66) to obtain

$$E = E_k - E_0 + 2 \frac{g_3^2(k)}{g_4(k)\rho_0(k)} \frac{1}{1+2g_4(k)\rho_0(k)\ln\frac{|E|}{2D}} \quad , \tag{69}$$

and this equation must be solved for E in order to get the bending of the dispersion curve. The result was written by Pitaevskij in the following form

$$E(k) = 2\Delta - \alpha e^{a(k-k_c)} \quad , \tag{70}$$

where α and a are parameters determined by those in (70). The bending of the spectrum shown in Fig. 2 has a strong resemblance with the one obtained by experiment [39]. In order to discuss that together with the part of the spectrum above $2\Delta_0$, further remarks are left of the end of this section.

The situation is somewhat more complicated in case of $g_4 < 0$. Below the threshold the dispersion curve of the two-roton bound state with helicity m=0 and the single particle spectrum has a crossing point if $g_3 = 0$. As a result of the Hamiltonian (64) hybridization is formed. The pole in the single-particle Green's function can be obtained easily if the expression (52) of the binding energy E_B for $g_3 = 0$ is introduced in (66), thus

$$E = E_k - 2\Delta_0 - 2\rho_0^{-1}(k)\frac{g_3^2}{g_4^2}\left[g_4(k)\rho_0(k) + \left(2\ln\frac{E}{E_B}\right)^{-1}\right] \tag{72}$$

At small momenta the spectrum of the bound state starts at K=0 which follows closely the curve of $g_3 = 0$ until the single-particle branch is approached. Then this spectrum turns upward and runs into the continuum. This is a typical example of level repulsion to avoid the crossing of curves with the same symmetry. The possible bound states with helicity $m \neq 0$ are not affected in this way. Furthermore, the single excitation branch before crossing the two-roton dispersion curve bends in the direction of higher momenta and at larger momentum values follows the bound state curve.

It is interesting to note that the nearer the dispersion curve goes to the bound state with $g_3 = 0$ the smaller the weight of the pole in the one-particle spectral function is. Thus, at large enough momenta the contribution of the flat part of the dispersion curve at $E \sim -E_B$ becomes negligible as it can be seen from the expression of the spectral function valid in this region

$$\rho_1(k, E<0) = \left[1 - \frac{g_3^2}{g_4^2}\frac{1}{\rho_0(k)}\left[1 + \frac{g_3^2}{g_4^2}\left(\ln\frac{|E|}{E_B}\right)^{-2}\right]^{-1}\right]\delta\left[E - E_\rho(k)\right] \quad , \tag{73}$$

where $E_\rho(k)$ denotes the root $E_\rho(k) = E$ of (72).

contributions from the energy regions $\omega < 2\Delta_0$ and $\omega > 2\Delta_0$ to the two-roton part of the spectrum is very sensitive on Γ, thus with increasing Γ the weight of the region $\omega \sim 2\Delta_0$ (but $\omega \sim 2\Delta_0$) is essentially enhanced, as one can see also in Fig. 6 of [41].

The results concerning the neutron scattering distribution can be summarized as follows:

The $S(k,\omega)$ has not been calculated, but we believe that the main features of the neutron scattering spectra are reflected by $\rho_1(k,\omega)$ fairly well. The inclusion of those processes in $S(k,\omega)$ in which that part of the density operator ρ comes into effect which contains operators of roton pairs may be important. As it has recently been suggested by Tutto [41], very likely these additive correction terms deform the spectrum toward larger energies due to a kinematical factor in the operator ρ. Therefore, it is important to emphasize that the fitting of the neutron data by $\rho_1(k,\omega)$ is instructive but in a rigorous sense it is not conclusive.

From the study of $\rho_1(k,\omega)$ one can conclude that the spectrum consist of two parts as the lower and upper branches shown in Fig. 2 and Fig. 6 of Cowley's lecture in the present volume. The lower branch at smaller momentum values starts with the phonon-roton part of the spectrum and, afterward, it shows the Pitaevskij bending due to the hybridization. If $g_4(k) < 0$ at larger momenta the bound state and the two-roton continuum can not be resolved by experiments. The weight of the lower branch there goes above the threshold $2\Delta_0$. The part of this branch below $2\Delta_0$ is very sensitive on the line width Γ of the rotons. Therefore, in the fitting the experimental data by $\rho_1(k,\omega)$ one can not use the procedure suggested earlier [10] that an effective Γ_{eff} is inserted into the theoretical expressions, which is $\Gamma_{eff} = \Gamma + \Gamma_{exp}$ where Γ_{exp} is the experimental broadening. Thus, one should calculate first $\rho_1(k,\omega)$ with Γ and then to take the convolution with the function of experimental broadening. The upper branch starts with the two-roton (and two-maxon etc.) contribution and getting nearer to the hybridization point it bends upward. On the lineshape the remarks made just above are valid. Furthermore, a definite level repulsion effect can be seen in the momentum range of the maxons where the lower branch is less far from the upper branch. Passing hybridization point the upper branch continuously goes over the single-particle free He^4 atom spectrum, which is, however, overdamped.

The problem concerning the sign of the interaction is left to the discussion.

VI. Conclusion

We may conclude that the main structure of the Raman spectra is understood on the basis of two-roton bound or resonance state concepts. The two branches in the neutron scattering spectra are explained by hybridization of the one- and two-excitation (or particle) spectrum, and that explanation reflects the rough behavior fairly well. According to the Raman spectrum the roton-roton interaction is attractive in the channel $\ell = 2$. Furthermore, the temperature dependence of the roton width indicates, that at larger momenta $k < _0 K < 2k_0$, several channels of the different helicity values must be effective (at least seven). Accepting, that the roton-roton interaction explains correctly the temperature dependence of the roton energy, similar conclusions can be drawn: Since the temperature

The behaviour above the threshold shows more interesting structure, namely, there are two interesting regions as $\omega \sim 2\Delta_0$ and $\omega \sim E(k)$. The one-particle spectral function can be obtained by taking the imaginary part of the one-particle Green's function (27) and by inserting the self energy given by (65) where F(k) is given by (49) and (50), hence

$$\rho_1(k,E>0)=g_3^2\rho_0(k)\frac{g_4^2\left[\pi^2+\left(\ell n\frac{E}{E_B}\right)^2\right]}{\left\{\left[g_4^2\rho_0(k)(E+2\Delta_0-E_k)+2g_4\rho_0(k)\right]\left[\pi^2+\left(\ell n\frac{E}{E_B}\right)^2\right]\right\}+g_3^2\ell n\frac{E}{E_B}^2+}$$
$$+(\pi\rho_0(k)g_3^2)^2 \quad , \qquad (74)$$

where it is assumed that $E>2\Delta_0$ and $\Gamma=0$.

In the case $\omega \sim E_k$ with $k>\frac{2}{3}k_0$ the spectrum goes very similarly as E(k) does, but there is a strong damping which is due, first of all, to the decay into two excitations. The spectral function has a Lorentzian form

$$\rho_1(k,E)=\frac{1}{\pi}\frac{\frac{1}{2\tau(k)}}{(E+2\Delta_0-E_k)^2+\left(\frac{1}{2\tau(k)}\right)^2} \quad , \qquad (75)$$

which can be obtained for (73) in the limit $E_k-2\Delta_0, E\gg E_B$. Furthermore δE_k is the shift of the real part of the pole E_k due to the coupling g_3 and the inverse lifetime is expressed according to the "golden rule" as

$$\frac{1}{\tau(k)}=2\pi(2g_3)^2\rho_2(k,E+2\Delta_0+E_k+\delta E_k) \quad . \qquad (76)$$

In the formal derivation of this result from (74) the relation (36) has been used.

The other part of the spectrum which can be obtained easily is where E(k) is far from $\omega \sim 2\Delta_0$, thus the region of the two-roton continuum. By making use of the approximation $\omega \sim 2\Delta_0$ and $|\omega-E_k|/E_B>1$ it is easy to obtain from (74) that

$$\rho_1(k,\omega)=(2g_4)^2\frac{\rho_2(k,\omega)}{[E(k)-\omega]^2} \quad . \qquad (77)$$

Thus at small or large enough momenta in the energy region $\omega \sim 2\Delta_0$, but $E>2\Delta_0$ the spectrum simply reflects the two-particle density of states with $g_4\neq 0$ but $g_3=0$ as it is expected on the basis of simple perturbation theory. That has an important consequence in these regions of small or very large momenta that the two-roton branch contains a relatively large contribution from energy region above $2\Delta_0$.

Finally, the effect of finite Γ for the rotons should be mentioned, where Γ has been discussed in section IV. In those parts of the spectrum, where the energy dependence in case $\Gamma=0$ is smooth enough, the broadening due to Γ does not lead to any remarkable effect. The situation is, however, different near to the two-roton bound state if $g_4<0$. In (73) the sharpness of the resonance comes into account in two different ways, as directly through the Dirac delta function and indirectly in its weight function. Thus, if Γ is taken into account, the weight function does not go to zero as $E \to -E_B$ in contrast with the case $\Gamma=0$. Therefore, as it has been pointed out by Tutto and Zawadowski [40], the ratio of the

dependence has a negative sign there must be a dominating attractive feature in the roton-roton interaction. On the basis of the momentum dependence of the bound state suggested by Pitaevskij and Fomin, it follows that at K=0 bound states with larger ℓ must exist. The neutron scattering provides information on the two-roton states only of helicity m=0. Thuś, from the dominating attractive behavior of the roton-roton interaction it is very likely that the interaction is attractive in the channel m=0, as well, but some accidental cancellation effects can not be ruled out.

In this way, two remarks can be made concerning the findings of Smith [42] et al. who fitted the neutron data by the expression $\rho_1(k,\omega)$ discussed in section IV. and suggested that the roton-roton interaction is mainly repulsive. Assuming that the explanation for the temperature dependence of the roton energy is correct, they are as follows:

(i) the roton-roton interaction may be repulsive in the channel of helicity m=0, but it is unlikely, because it must be on a dispersion curve which starts at a bound state at K=0. This follows from the fact, that the bound state at K=0 has a component of m=0.

(ii) the interaction is attractive for m=0 also, but either the $\rho_1(k,\omega)$ is not good enough to represent $S(k,\omega)$ or the improvement in the fitting procedure and the experimental accuracy may lead to a change of the previous conclusion. *

Further neutron scattering measurements and theoretical efforts to calculate $S(k,\omega)$ or the improvement in the fitting procedure and the experimental accuracy may lead to a change of the previous conclusion.

The theoretical efforts to calculate the interaction on the basis at some microscopic or semimicroscopic models are promising [43] and the works of Roberts, Donnelly and Pardee [44,45] based on a roton-roton interaction of dipole type look like a good starting point. The only firm experimental information on the structure of the interaction for K≠0, is, however that at least seven helicity channels are involved: thus the interaction must strongly depend on the angle between the momentum planes before and after the scattering. Such a dependence and a strong enough coupling can be produced by a phonon exchange mechanism. There is, however, no ground to exclude the role of other excitations from the formation of the roton-roton coupling.

We should like to express our gratitude to Dr. I. Tüttő for the discussions which helped to clarify several points.

* See KFKI preprint by I. Tüttő and A. Zawadowski

References

1. L. D. Landau, J. Phys. Ussr 5, 71 (1941); 11 91 (1947).
2. L. P. Pitaevskij, Zh. Eksperim. i Theor. Fiz. 36 11 68 (1959) Sov. Phys. JETP 9, 830 (1959); Usp. Fiz. Fauk 88, 409 (1966) Sov. Phys. Usp. 9, 197 (1966).
3. A. D. B. Woods, in Quantum Fluids, edited by D. F. Brewer (North-Holland, Amsterdam, 1966.) p. 242.
4. L. D. Landau and I. M. Khalatnikov, in Collected Papers of Landau, edited by D. Fer Haar (Gordon and Breach, New York, 1967.) pp. 494 and 511.
5. T. J. Greytak and James Yan, Phys. Rev. Lett. 22, 987 (1969).
6. A. D. B. Woods and R. A. Cowley, Can. J. Phys. 49, 177 (1970).
7. F. Iwamoto, Progr. Theoret. Phys. (Kyoto) 44, 1121 (1970).
8. J. Ruvalds and A. Zawadowski, Phys. Rev.. B. 2, 1172 (1970).
9. F. Iwamoto, Prog. Theoret. Phys. (Kyoto) 44, 1121 (1970).
10. A. Zawadowski, J. Ruvalds and J. Solana, Phys. Rev. A 5, 399 (1972).
11. J. W. Halley, Phys. Rev. 181, 338 (1969).
12. M. J. Stephen, Phys. Rev. 186, 279 (1969).
13. D. Baeriswyl. PhD Thesis at University of Geneva, 1974.
14. A. Miller, D. Pines and P. Noxieres, Phys. Rev. 127, 1452 (1962).
15. A. D. B. Woods and R. A. Cowley, Rep. Prog. Phys. 36, 1135 (1973).
16. R. L. Woerner and T. L. Greytak, J. Low. Temp. Phys. 13 149 (1973).
17. D. Baereswyl, Phys. Lett. 41A, 297 (1972).
18. R. P. Feynmann and M. Cohen, Phys. Rev. 102, 1189 (1956).
19. L. P. Pitaevskij and I. A. Fomin, Zh. Eksperim. Teor. Fiz. 65, 2516 (1973). Sov. Phys. JETP 38, 1257 (1974).
20. A. D. B. Woods, P. A. Hilton, R. Scherm and W. G. Stirling, J. Phys. C: Solid State Phys. 10, L45 (1977).
21. C. A. Murray, R. L. Woerner and T. J. Greytak, J. Phys. C. 8, L90 (1975).
22. D. Baereswyl and J. Jackle, Helv. Physica Acta 44, 554 (1971).
23. I. Tütto, A. Zawadowski, to be published
24. I. Tütto, to be published

25. O. W. Dietrich, E. H. Graf, C. H. Huang and L. Passell, Phys. Rev. A5, 1377 (1972).

26. J. Ruvalds, I. Tutto and A. Zawadowski (unpublished)

27. J. Wilks, The Properties of Liquid and Solid Helium Clarendon Univ. Press, Oxford, 1967 p. 177.

28. T. J. Greytak and J. Yan in Proceedings of the Twelfth International Conference on Low Temperature Physics, Kyoto, September 1970, edited by E. Kanda

29. J. Ruvalds, Phys. Rev. Lett. 27, 1769 (1971).

30. I. Tütto, P: Low Temp. Phys. 11, 77 (1973).

31. J. Solana, thesis at University of Virginia 1971, unpublished and see also in Ref. 35.

32. K. Nagai, K. Nojima and A. Hatano, Prog. Theoret. Phys. (Kyoto) 46, 335 (1972).

33. J. Yan and M. Stephens, Phys. Rev. Letters 27, 482 (1971).

34. I. A. Fomin. Zh. Eksperim. i. Teor. Fiz. 60, 1178 (1971) Sov. Phys. JETP 33, 637 (1971).

35. J. Solana, V. Celli, J. Ruvalds, I. Tutto and A. Zawadowski, Phys. Rev. A6, 1665 (1972).

36. K. Nagai Progr. Theoret. Phys. 49, 46 (1973).

37. K. Kebukawa, Progr. Theoret. Phys. (Kyoto) 39, 388 (1973).

38. F. Iwamoto, Prog. Theor. Phys. (Kyoto) 44, 1121 (1970). see also C. P. Enz, Phys. Rev. A6, 1605 (1972).

39. E. H. Graf, V. J. Minkiewicz, 11. Bjerrum Moller and L. Passel, Phys. Rev. A10, 1748 (1974).

40. I. Tütto and A. Zawadowski (to be published)

41. A. J. Smith, R. A. Cowley, A. D. B. Woods, W. G. Stirling and P. Martel, J. Phys. C 10, 543 (1977).

42. I. Tütto, seminar given at this school (unpublished)

43. D. K. Lee, Phys. Rev. 162, 134 (1967).

44. P. H. Roberts and R. J. Donelly, Tour. Low. Temp. Phys. 15, 1 (1974).

45. P. H. Roberts and W. J. Pardee, J. Phys. A. 7 11 (1974).

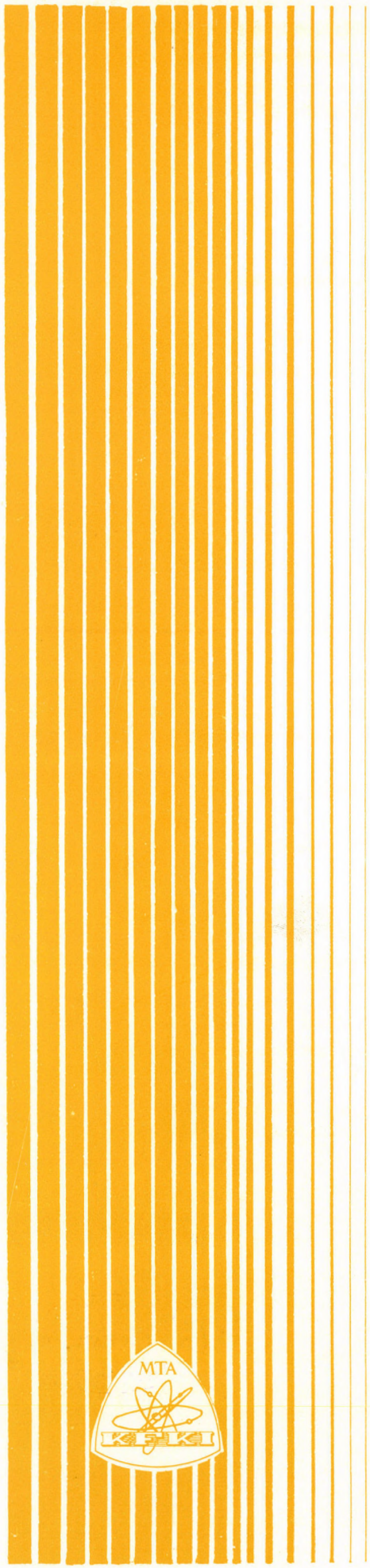

Kiadja a Központi Fizikai Kutató Intézet
Felelős kiadó: Vasvári B.
Szakamai lektor: Sólyom Jenő
Nyelvi lektor: Sólyom Jenő
Példányszám: 170 Törzsszám: 78-131
Készült a KFKI sokszorositó üzemében
Budapest, 1978. február hó